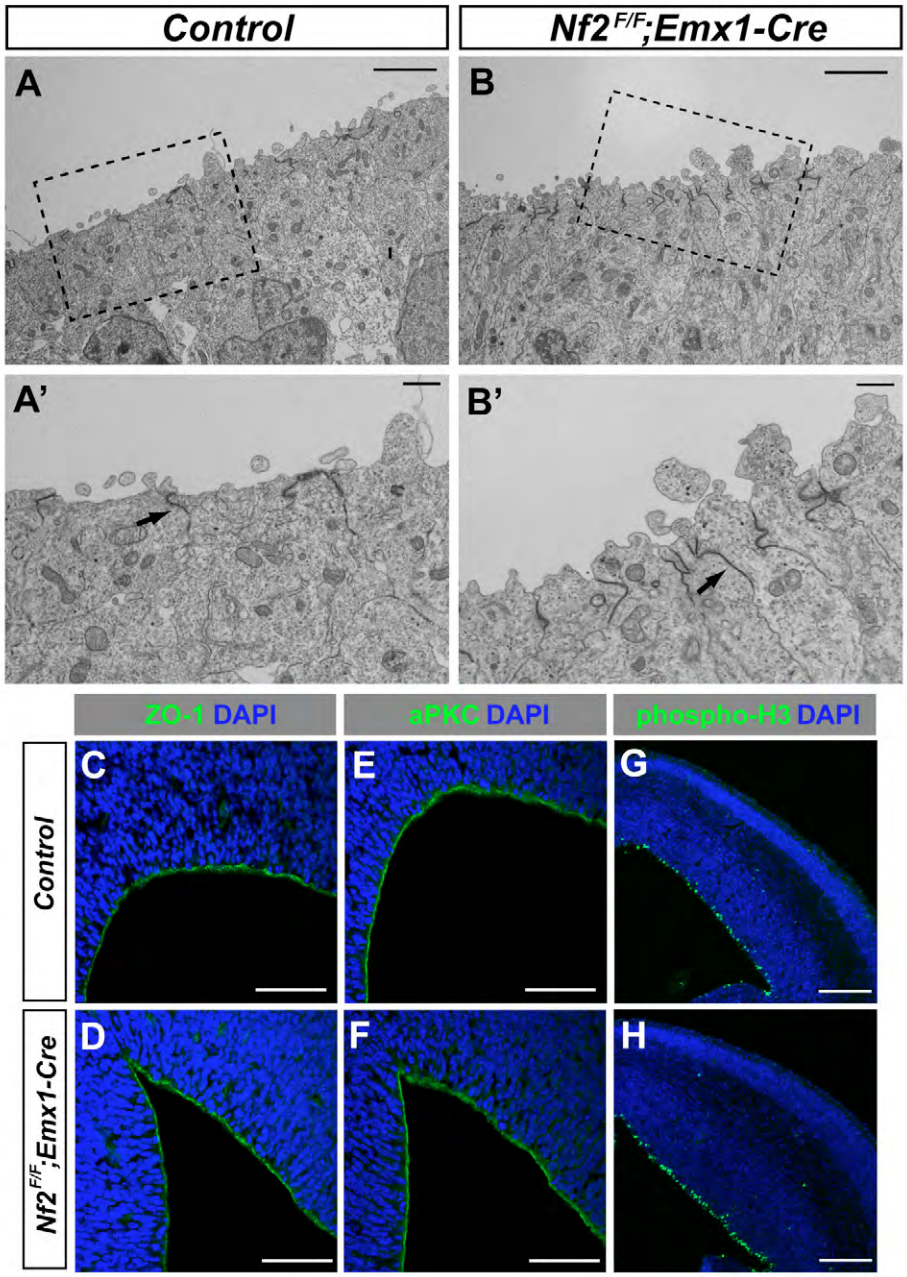

Fig. S1. The apical junctions and polarity of NPCs are unaffected in *Nf2* mutant dorsal telencephalons. (**A-B′**) Transmission electron microscopy of E15.5 brains show that the apical junctions (arrows) are intact in the *Nf2$^{F/F}$;Emx1-Cre* dorsal telencephalon. A′ and B′ are magnified views of the dashed boxes in A and B, respectively. (**C-H**) Immunostaining shows that, in the E15.5 *Nf2$^{F/F}$;Emx1-Cre* cortex, the apical junctional component ZO-1, the apical polarity protein aPKC and mitotic NPCs (labeled by phospho-H3) are all properly localized at the apical/ventricular surface. Scale bars: 4 μm in A,B; 1 μm in A′,B′; 50 μm in C-F; 200 μm in G,H.

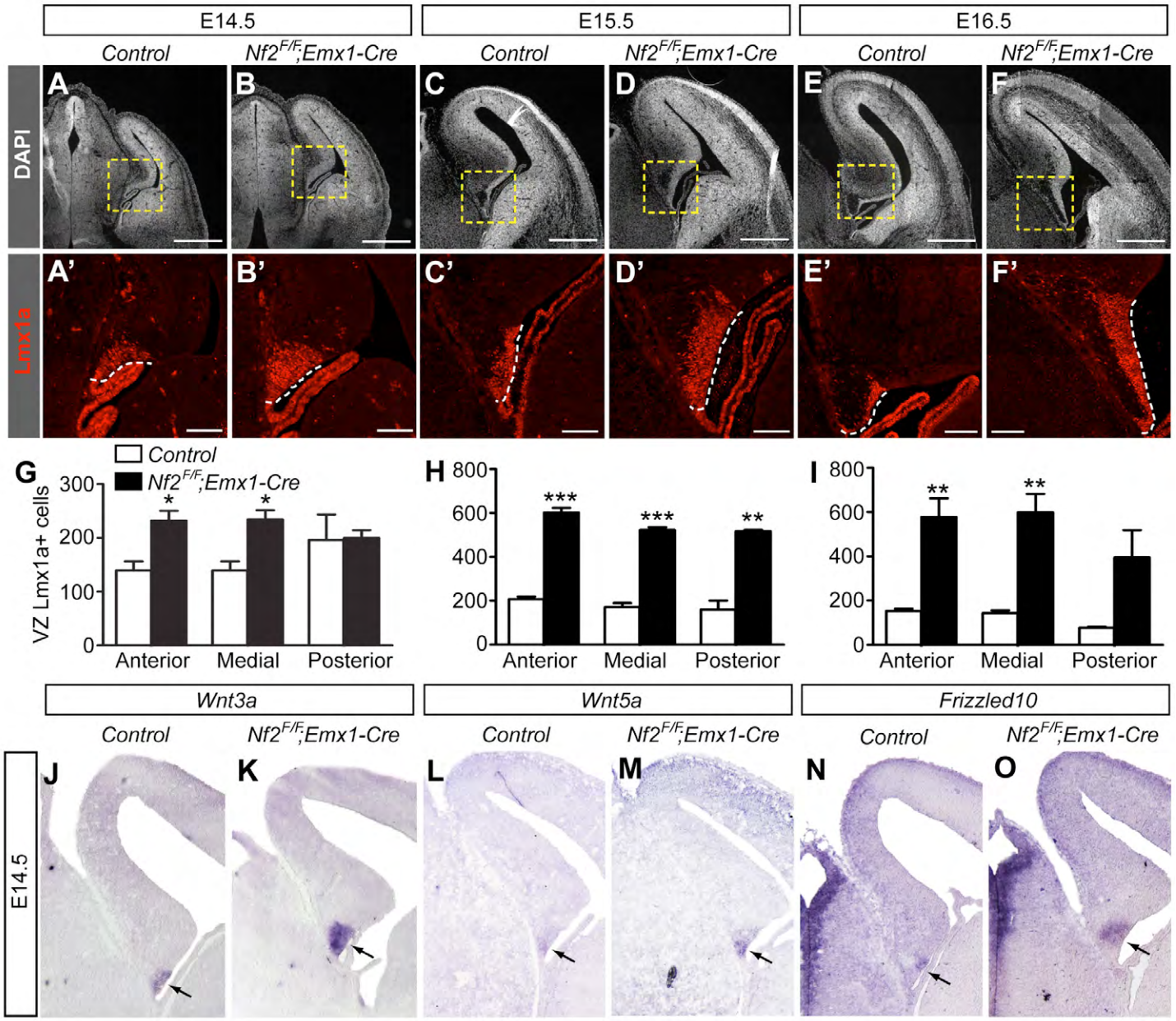

Fig. S2. The cortical hem is markedly enlarged in *Nf2* mutant embryos. (**A-F′**) Images of the dorsal telencephalon (shown by DAPI staining) and cortical hem (labeled by Lmx1a, delineated by dashed lines) show that the hem is markedly enlarged in *Nf2$^{F/F}$;Emx1-Cre* embryos. (**G-I**) Quantifications of the number of VZ Lmx1a^{+} hem cells per section along the anterior-posterior axis of the hem structure at E14.5 (G), E15.5 (H) and E16.5 (I). Values are mean ± s.e.m. of three embryos. **P*<0.05, ***P*<0.01, ****P*<0.001. (**J-O**) *In situ* hybridizations on E14.5 brain sections show that the *Nf2$^{F/F}$;Emx1-Cre* hem expresses the hem markers *Wnt3a*, *Wnt5a* and *Fzd10*. Scale bars: 500 μm in A-F; 100 μm in A′-F′.

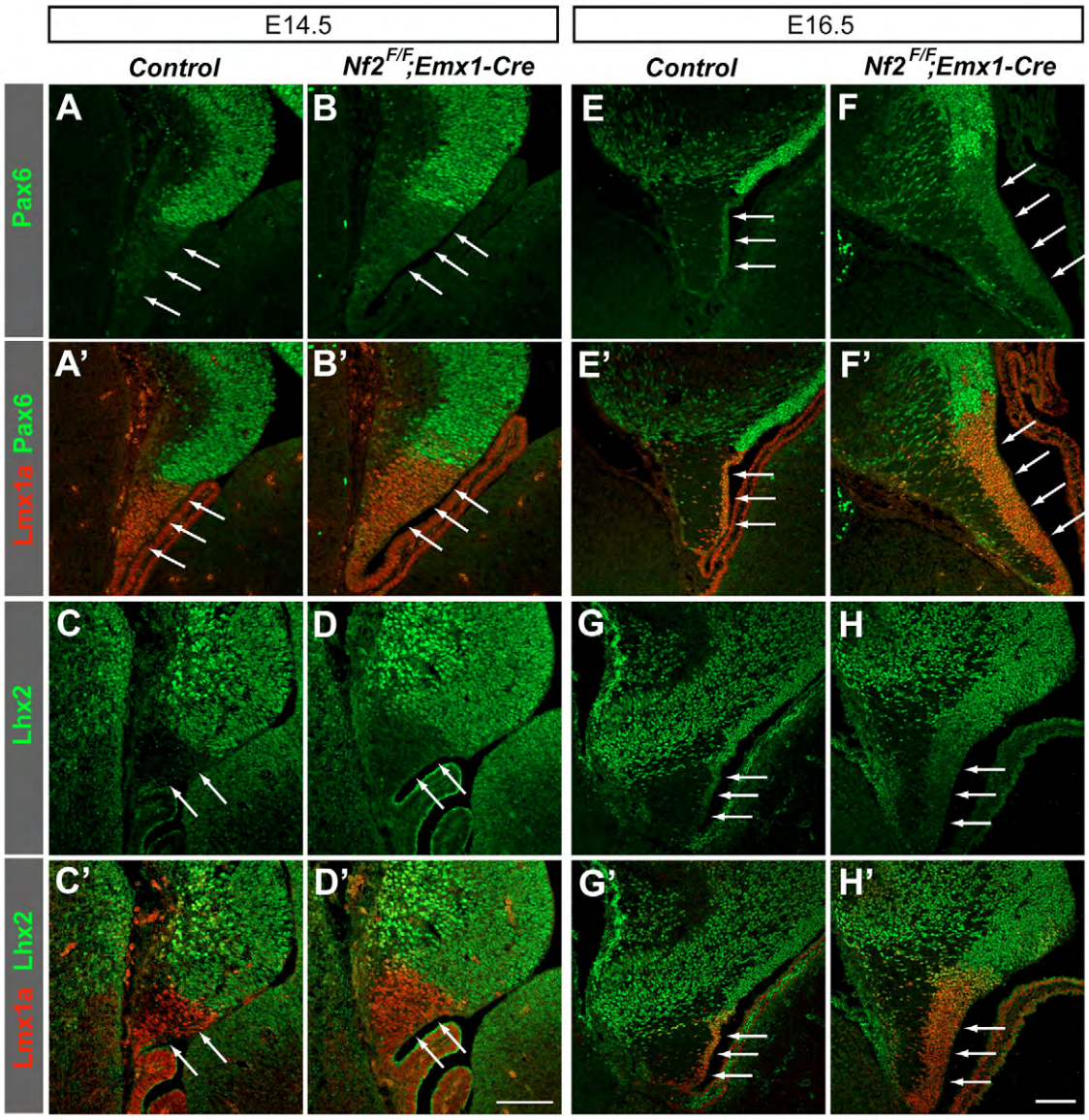

Fig. S3. The cortex and hem fates are properly specified and maintained in *Nf2* mutants. (**A-H′**) Co-immunostaining for the hem marker Lmx1a with the cortex markers Pax6 and Lhx2 shows no overlapping of the hem and cortex markers in *Nf2$^{F/F}$;Emx1-Cre* brains at E14.5 and E16.5. Arrows point to the hem. Scale bars: 100 μm.

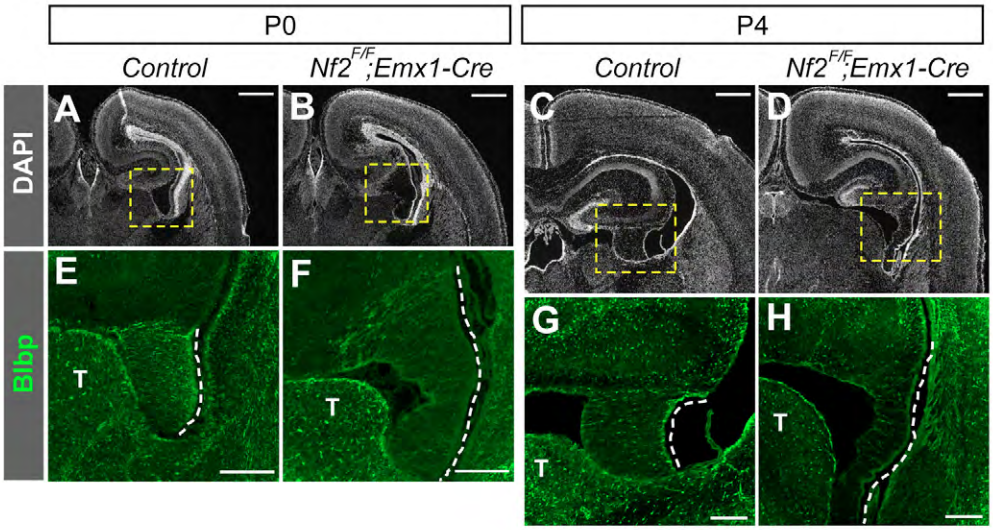

Fig. S4. Blbp expression fails to be upregulated at the hem of *Nf2* mutants. (**A-H**) Images of the dorsal telencephalon (shown by DAPI staining, A-D) and hem (delineated by dashed lines, E-H) show that Blbp expression remains low at the *Nf2$^{F/F}$;Emx1-Cre* hem at P0 and P4 (F,H versus E,G). E-H are magnified views of the dashed boxes in A-D, respectively. T, thalamus. Scale bars: 500 μm in A-D; 200 μm in E-H.

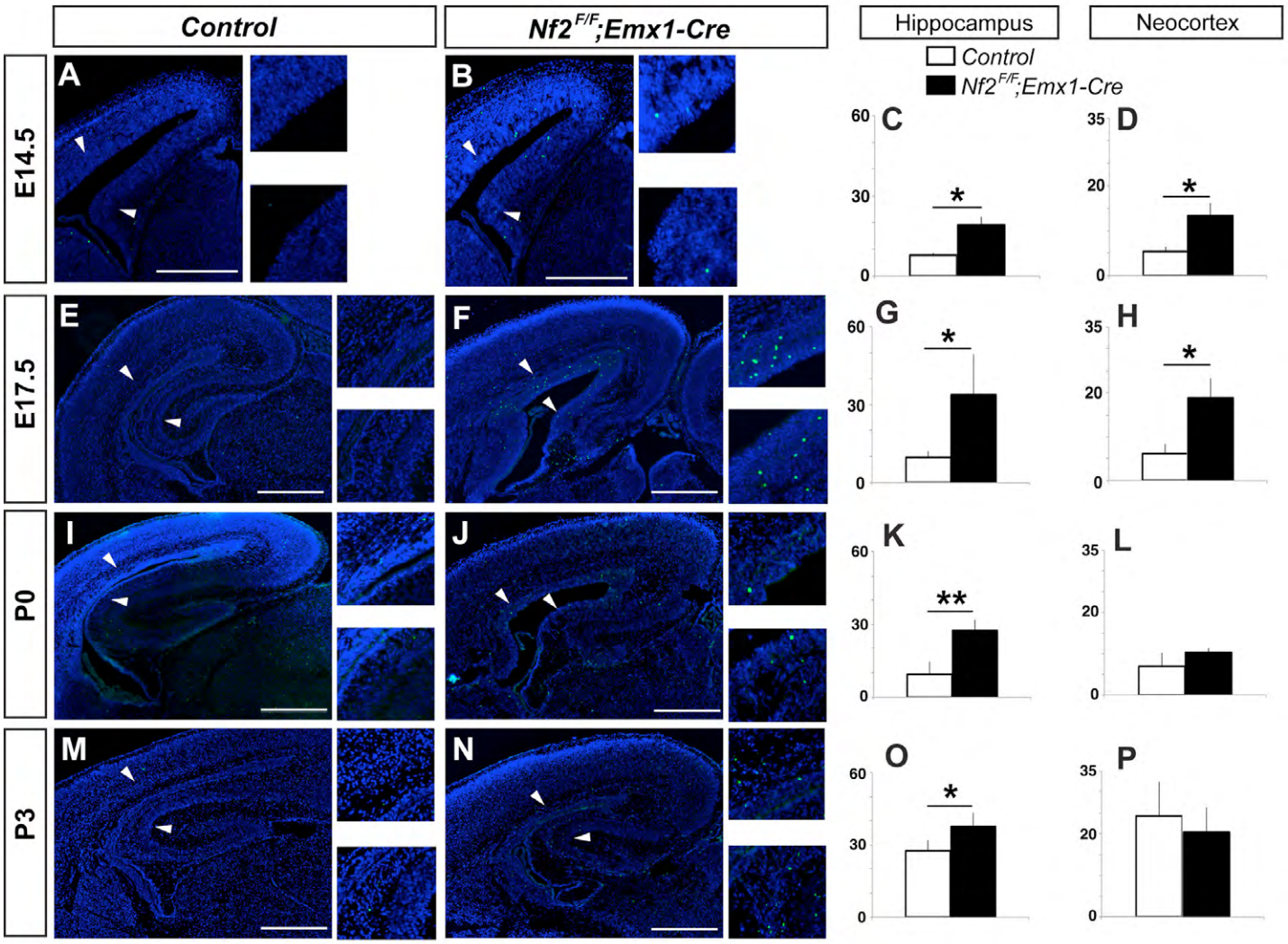

Fig. S5. Increased cell death in the dorsal telencephalon of *Nf2* mutants during development. (**A-P**) TUNEL assays (green signal) on E14.5, E17.5, P0 and P3 brain sections show increased cell death in the hippocampus of *Nf2$^{F/F}$;Emx1-Cre* brains at all these stages (C,G,K,O) and in the neocortex at E14.5 and E17.5 (D,H). Small panels on the right of each large panel are magnified views of the neocortical (top) and hippocampal (bottom) regions indicated by the arrowheads. Values in bar charts are the number of TUNEL$^+$ cells per section ± s.d. (*n*=3 animals). Blue signals are DAPI staining. Scale bars: 500 μm.

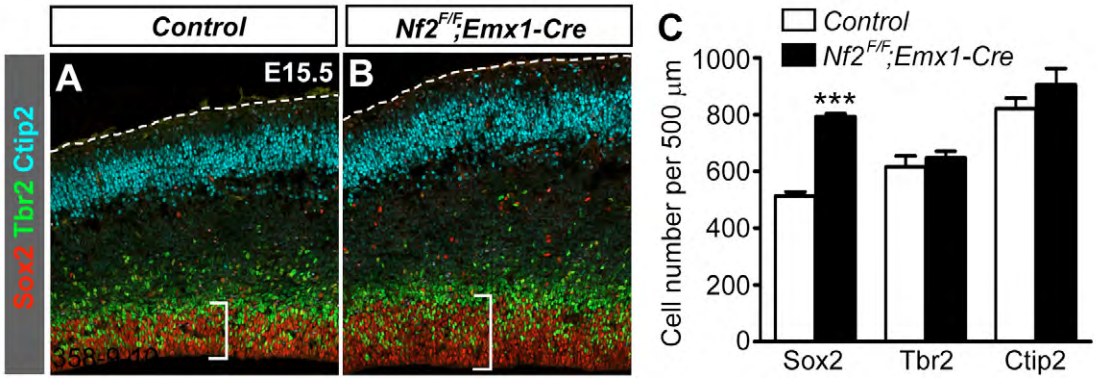

Fig. S6. Loss of Nf2 results in an expansion of the neocortical neural progenitor population. (**A**,**B**) Immunostaining with the NPC marker Sox2, the intermediate progenitor marker Tbr2, and the deep layer cortical neuron marker Ctip2 shows expansion of the NPC population in the E15.5 *Nf2$^{F/F}$;Emx1-Cre* neocortex. (**C**) The numbers of Tbr2$^+$ and Ctip2$^+$ cells are not affected by *Nf2* deletion. Note that Sox2$^+$ Tbr2$^-$ cells are counted as the 'Sox2' category. Values are the mean number of positive cells per 500 μm of neocortical column ± s.e.m. (*n*=3 embryos). ***P<0.001.

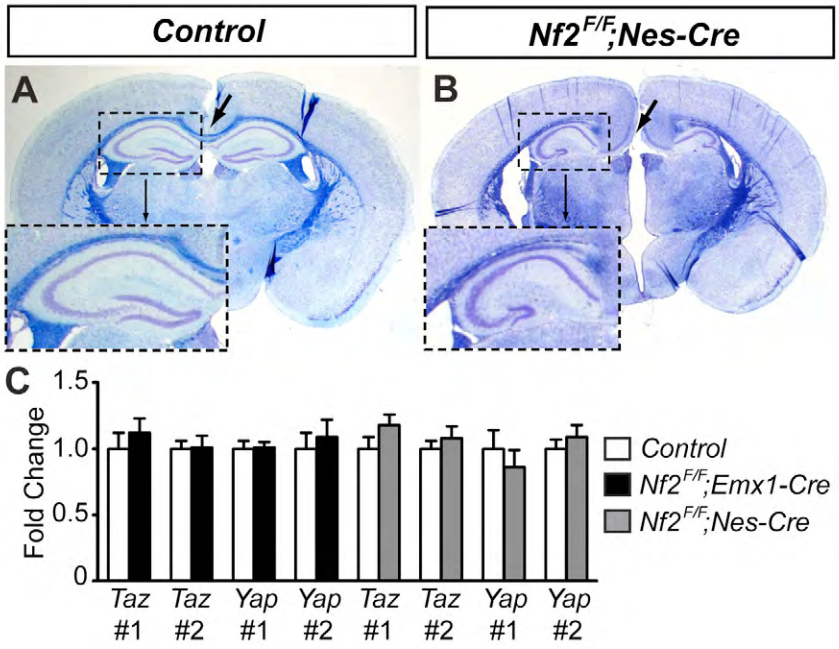

Fig. S7. Nf2 loss does not affect *Yap* and *Taz* mRNA levels. (**A**,**B**) The dorsal telencephalon of *Nf2$^{F/F}$;Nes-Cre* mice has similar phenotypes to that of *Nf2$^{F/F}$;Emx1-Cre* mice. Luxol Blue staining for myelinated axons (blue) and Cresyl Violet for neuronal cell bodies (purple) show dysgenesis of the corpus callosum (arrows) and malformation of the hippocampus (dashed boxes) in 2-month-old *Nf2$^{F/F}$;Nes-Cre* mice (B), which are similar to those seen in *Nf2$^{F/F}$;Emx1-Cre* mice. (**C**) Loss of Nf2 does not affect the levels of *Yap* and *Taz* transcripts. Quantitative RT-PCR analysis shows similar levels of *Yap* and *Taz* transcripts in E13.5 *Nf2$^{F/F}$;Emx1-Cre* dorsal telencephalons and *Nf2$^{F/F}$;Nes-Cre* whole brains when compared with their corresponding controls. Two sets of PCR primers were used for each gene (#1 and #2). Values are mean ± s.e.m. of three embryos per genotype.

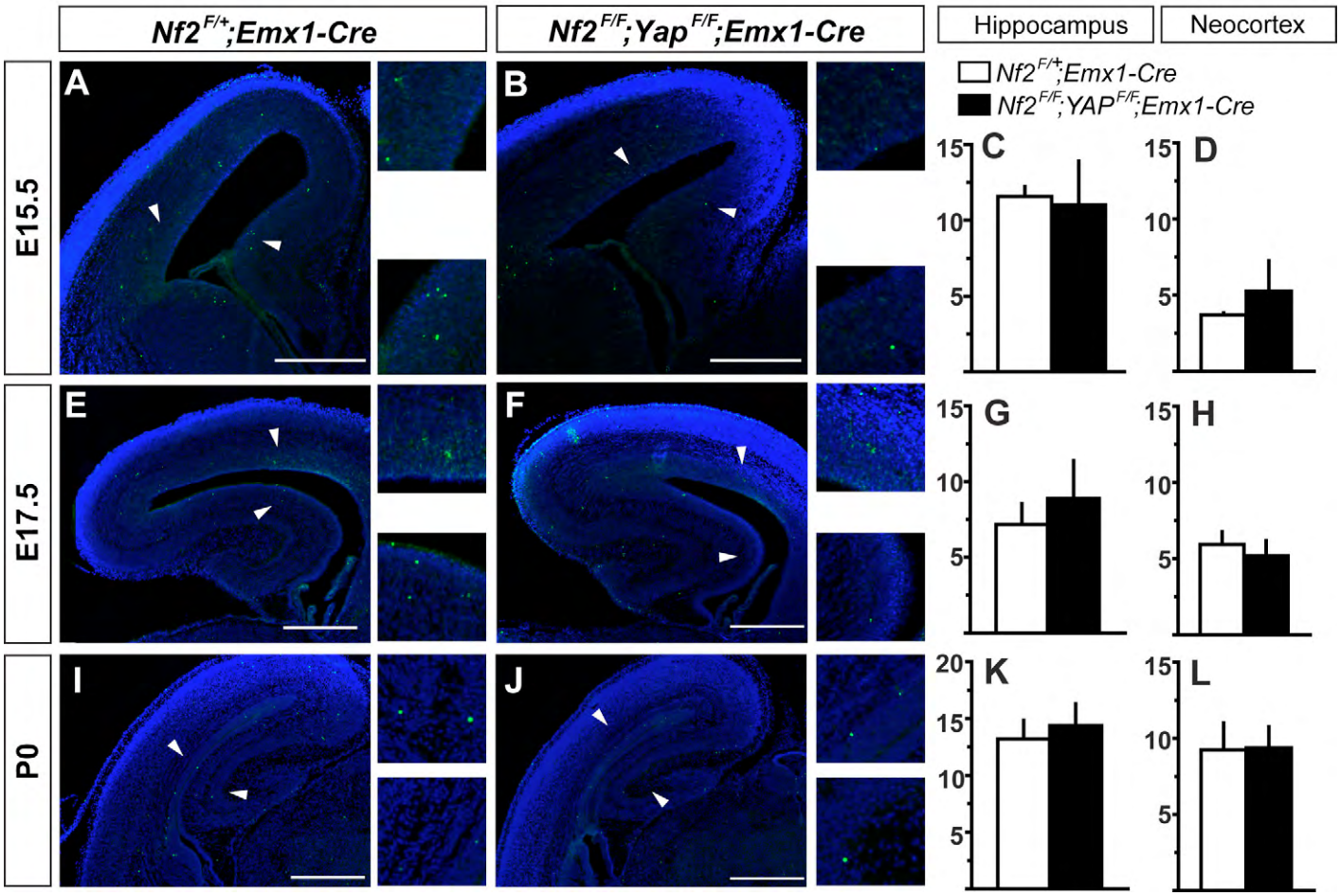

Fig. S8. ***Yap*** **deletion suppresses the cell death phenotype of** ***Nf2*** **mutants.** (**A-L**) TUNEL assays (green signal) on E15.5, E17.5 and P0 brain sections showing no increase in cell death in *Nf2*$^{F/F}$;*Yap*$^{F/F}$;*Emx1-Cre* brains at any of these stages. Small panels on the right of each large panel are magnified views of the neocortical (top) and hippocampal (bottom) regions indicated by the arrowheads. Values in bar charts are the number of TUNEL^{+} cells per section ± s.e.m. (*n*=3 animals). Blue signals are DAPI nuclear staining. Scale bars: 500 μm.

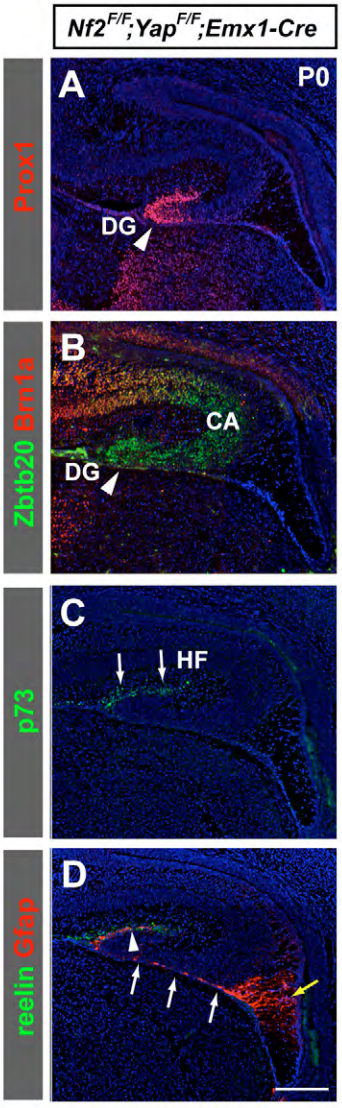

Fig. S9. *Yap* deletion sometimes partially rescues the hippocampal defects associated with Nf2 loss. Some *Nf2$^{F/F}$;Yap$^{F/F}$;Emx1-Cre* brains exhibit a partial rescue of the hippocampal defects found in *Nf2$^{F/F}$;Emx1-Cre* brains. (**A**) The dentate gyrus (DG), although still smaller than in the control, shows distinguished double blades (arrowhead). (**B**,**C**) The pyramidal cell layer (CA) labeled by Zbtb20/Brn1a and the hippocampal fissure (HF) labeled by p73 are improved compared with those in *Nf2$^{F/F}$;Emx1-Cre* brains, albeit still smaller than those in the control. (**D**) Gfap^{+} glial shaft (white arrows) and fibers (arrowhead) are present at the subpial space, although ectopic fibers are still found at the hem (yellow arrows). Blue signals are DAPI nuclear staining. Scale bar: 200 μm.

Table S1. Primary antibodies for immunostaining

Antibody	Host species	Vendor	Catalog #
Nf2/merlin	rabbit	Santa Cruz	sc-332
Nf2	rabbit	Sigma	HPA003097
β-catenin (Alexa 647 conjugated)	mouse	Cell Signaling	9587
ZO-1 (Alexa 488 conjugated)	mouse	Invitrogen	339188
aPKC	rabbit	Santa Cruz	sc-216
Phospho-histone H3	rabbit	Chemicon	06-570
Lmx1a	goat	Santa Cruz	sc-54273
Lmx1a	rabbit	Sigma	HPA030088
Ki67	rabbit	Vector Labs	VP-RM04
BrdU	rat	Abcam	ab6326
Pax6	rabbit	Covance	PRB-278P
Lhx2	goat	Santa Cruz	sc-19342
RC2	mouse	Developmental Studies Hybridoma Bank	RC2
Blbp	rabbit	Millipore	ABN14
Sox2	goat	Santa Cruz	sc-17320
Sox2	rabbit	Cell Signaling	3728
Tbr2	rabbit	Abcam	ab23345
Tbr2 (Alexa 647 conjugated)	rat	eBiosciences	51-4875
Ctip2	rat	Abcam	ab18465
YAP (pS127)	rabbit	Cell Signaling	4911
Zbtb20	rabbit	Sigma	HPA016815
Prox1	goat	R&D Systems	AF2727
Prox1	rabbit	Millipore	AB5475
p73	rabbit	Santa Cruz	sc-7957
Reelin	goat	R&D Systems	AF3820
Calretinin	rabbit	Millipore	AB149
Gfap	rabbit	Dako	Z0334
Nestin	goat	R&D Systems	AF2736
Brn1a	goat	Santa Cruz	6028-R

Table S2. Quantitative RT-PCR primers

Primer	Sequence
Steap1 forward	CTATTCCATCTGTGAGCGACTC
Steap1 reverse	ACATCTACCCATTTATTCCAGGC
Ctgf forward	CCTGCCATTACAACTGTCCT
Ctgf reverse	GTTCGTGTCCCTTACTTCCTG
Cyr61 forward	CCGCCTGGTGAAAGAGAC
Cyr61 reverse	GGGATTTCTTGGTCTTGCTG
Pkp2 forward	GCAGACCATGTACCAGTATCC
Pkp2 reverse	CGTTCTGAAGTTTGAGCAGTTG
Clusterin forward	TGGACACAGTGGCGGAGAA
Clusterin reverse	TCCGCACGGCTTTTCCT
Wwc2 forward	GTGCAGATAGGACTCAGATACG
Wwc2 reverse	AGCAGAGCGACCCTAAAATAC
Ajuba forward	AGCCTCTACCACACCCAG
Ajuba reverse	ACAGACACAGCACTTCTCAG
Amotl2 forward	AGATGGAGACTGTACTGAGGG
Amotl2 reverse	GAGCCGCTGGATTTCATTTTC
YAP#1 forward	ACCAATAGTTCCGATCCCTTTC
YAP#1 reverse	TGTCTCCTGTATCCATTTCATCC
YAP#2 forward	ACCATAAGAACAAGACCACATCC
YAP#2 reverse	CTTCACTGGAGCACTCTGAG
TAZ#1 forward	GAGAGGATTAGGATGCGTCAAG
TAZ#1 reverse	GGATCTGAGCTACTGTTGGTG
TAZ#2 forward	AGACTTCCTCAGCAACATGG
TAZ#2 reverse	AGTCCCGAGGTCAACATTTG

Table S3. Microarray analysis

Download Table S3